Donor-Donor Energy Migration for Determining Intramolecular Distances in Proteins: I. Application of a Model to the Latent Plasminogen Activator Inhibitor-1 (PAI-1)

Jan Karolin,* Ming Fa,# Malgorzata Wilczynska,# Tor Ny,# and Lennart B.-Å. Johansson*
*Department of Physical Chemistry and #Department of Medical Biochemistry and Biophysics, Umeå University, S-901 87 Umeå, Sweden

ABSTRACT A new fluorescence spectroscopic method is presented for determining intramolecular and intermolecular distances in proteins and protein complexes, respectively. The method circumvents the general problem of achieving specific labeling with two different chromophoric molecules, as needed for the conventional donor-acceptor transfer experiments. For this, mutant forms of proteins that contain one or two unique cysteine residues can be constructed for specific labeling with one or two identical fluorescent probes, so-called donors (*d*). Fluorescence depolarization experiments on double-labeled Cys mutant monitor both reorientational motions of the *d* molecules, as well as the rate of intramolecular energy migration. In this report a model that accounts for these contributions to the fluorescence anisotropy is presented and experimentally tested. Mutants of a protease inhibitor, plasminogen activator inhibitor type-1 (PAI-1), containing one or two cysteine residues, were labeled with sulfhydryl specific derivatives of 4,4-difluoro-4-borata-3a-azonia-4a-aza-*s*-indacence (BODIPY). From the rate of energy migration, the intramolecular distance between the *d* groups was calculated by using the Förster mechanism and by accounting for the influence of local anisotropic orientation of the *d* molecules. The calculated intramolecular distances were compared with those obtained from the crystal structure of PAI-1 in its latent form. To test the stability of parameters extracted from experiments, synthetic data were generated and reanalyzed.

INTRODUCTION

The Förster mechanism of electronic energy transfer (Förster, 1948) has been studied and applied in a large number of reports. According to Förster, the rate of energy transfer (ω) between donor (d) and acceptor (a) molecules separated by a distance R is proportional to $1/R^6$. Because the rate of energy transfer depends on the distance between the interacting molecules, one obvious application would be as a spectroscopic ruler. To examine the process of energy transfer, several bichromophoric da systems have been synthesized (Berberan-Santos and Valeur, 1991; Kaschke et al., 1990; Latt et al., 1965; van der Meer et al., 1994; Stryer and Haugland, 1967; Valeur, 1989; Valeur et al., 1989). The principal structure of such a system, as well as the transfer process, is illustrated in Fig. 1 *A*. The d and the a molecules are covalently bound to a macromolecule (P) by means of a linker molecule denoted by L. For most da systems the excitation energy is irreversibly transferred from the excited donor molecule to a ground-state acceptor molecule, as is indicated in Fig. 1 *A*. Because of the rate of energy transfer dependence on the distance between the interacting chromophores, one application has been distance determinations in macromolecular systems.

To apply da transfer to the measurement of distances in proteins, the d and a molecules must be specifically attached at two sites. In practice, this is an extremely difficult task. Although there are several reactive fluorescent molecules that can be used to label the amine and the thiol groups (Lakey et al., 1991; Strandberg et al., 1994; Haugland, 1996), there is still a very big problem in achieving specific labeling. Because the amine groups are present in several amino acids and in one terminal end of the polypeptide chains, the problem of specificity is obvious. Even if one obtains a stochiometric labeling ratio, the exact positions of the chromophores are usually unknown (Stratikos and Gettins, 1997). This problem can be circumvented by using the reactive properties of the much less abundant thiol groups. Furthermore, by using site-specific mutagenesis, a protein can be modified to contain one or two cysteine residues at well-defined positions. The problem, however, still remains of achieving a specific labeling of the sulfhydryl groups with two different chromophores, i.e., a donor and an acceptor. In contrast, the specific labeling of a protein in two positions with the same kind of fluorophores is a straightforward task, i.e., with two donor molecules. If the photophysical properties of the donors are the same in both sites, the excitation energy of such a bichromophoric system is reversibly transferred between the fluorescent moieties. This process is usually referred to as donor-donor (dd) energy migration (DDEM), which can only be monitored by fluorescence anisotropy. The aim of this work is to show how reliable distance information can be extracted from the rate of DDEM in double-labeled proteins.

Until recently (Johansson et al., 1996a; Aleshkov et al., 1996), studies of DDEM between identical fluorophores have been very rare, and usually vitrified samples have been examined (Moog et al., 1984; Ikeda et al., 1988; Bastiaens et al., 1991; Kalman et al., 1991). A likely reason is that, in

Received for publication 6 February 1997 and in final form 21 October 1997.

Address reprint requests to Dr. Lennart B.-Å. Johansson, Department of Physical Chemistry, Umeå University, S-901 87 Umeå, Sweden. Tel.: 46-90-786-51-49; Fax: 46-90-786-77-79; E-mail: lennart.johansson@chem.umu.se.

0006-3495/98/01/11/11 $2.00

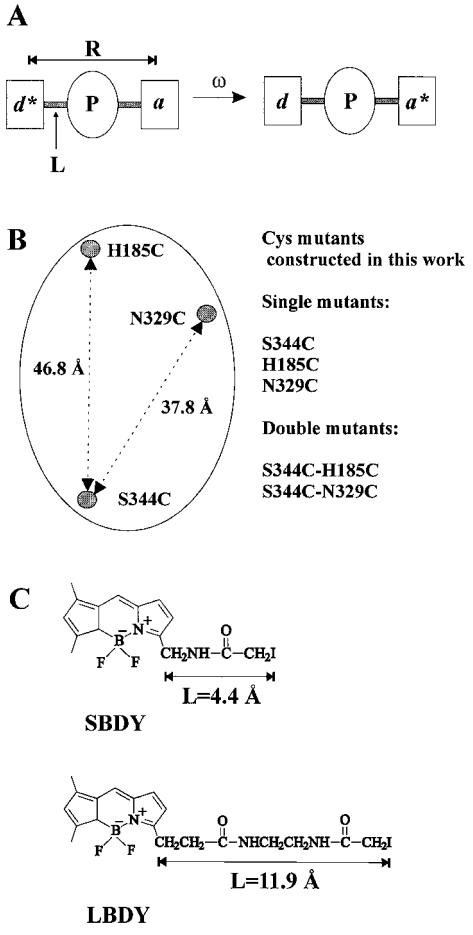

FIGURE 1 (*A*) Schematic of a bichromophoric system. Energy is transferred from an excited donor molecule (*d**) to an acceptor molecule (*a*) in its electronic ground state. The chromophores are attached to a macromolecule (P) by a linker (L). The rate for energy transfer (ω) depends on the distance (R) between the *da* molecules. (*B*) The approximate locations of the mutated positions in latent PAI-1 are illustrated, together with distances obtained by inspection of the crystal structure. The distances given are between the C_α atoms of the mutated amino acid. The position S344C was selected to be common for both distances. (*C*) Structure formulas of *N*-(4,4-difluoro-5,7-dimethyl-4-bora-3a,4a-diaza-*s*-indacene-3-yl)methyl)-iodoacetamide (SBDY) and *N*-(4,4-difluoro-5,7-dimethyl-4-bora-3a,4a-diaza-*s*-indacene-3-propionyl)-*N*′-(iodoacethylene-diamine) (LBDY) used in this work. The distances of the fully stretched linkers were determined from molecular models.

addition to energy migration, reorientational motions of the d molecules will also contribute to the fluorescence anisotropy experiment. In this work we present and test a model for the fluorescence anisotropy that accounts for both energy migration and molecular reorientation within a protein. The validity of the model is examined by comparing the distance between the fluorophoric moieties obtained form the migration rate and that estimated from the x-ray structure. As a model system we have used the latent form of plasminogen activator inhibitor type-1 (PAI-1), which is a protease inhibitor that belongs to the serpin family of inhibitors. Because PAI-1 lacks cysteine residues, substitution mutants containing one or two unique cysteines for labeling were constructed. After labeling with sulfhydryl-specific derivatives of 4,4-difluoro-4-borata-3a-azonia-4a-aza-*s*-indacence (BODIPY), the mutants reveal biochemical characteristics very similar those of the wild type of PAI-1 (Strandberg et al., 1994; Fa et al., 1995; Aleshkov et al., 1996).

To determine one intramolecular distance with the DDEM method, three Cys mutant forms are needed. For the PAI-1 system these mutants, a double and the corresponding single mutants, were selected by inspection of the crystal structure of the latent form of the protein. The distances studied in this work are illustrated in Fig. 1 *B*. Because one position is chosen to be common with both distances, five different mutants have been constructed. The distances indicated in Fig. 1 *B* are between the C_α atoms of the mutated amino acids. In the DDEM experiments, as well as in energy transfer experiments, the distance obtained is that between the chromophoric groups. Because these groups are attached to the protein by a linker of specific length, a detailed comparison with the crystal structure at an atomic resolution is not possible. To investigate the influence of the linker on the distances determined, we have used two derivatives of BODIPY that differ only in the length of the linker (see Fig. 1 *C*).

The different Cys-labeled forms of PAI-1 were investigated by using time-resolved polarized fluorescence spectroscopy. To separate contributions from DDEM and reorientational motions in the data analysis, a combination of experimental results obtained for the three mutants forms were used. As an independent test of the stability of parameters extracted from data analysis, synthetic data have been generated and reanalyzed. A detailed description of this procedure is presented.

MATERIALS AND METHODS

The fluorescent probe molecules

The sulfhydryl specific derivatives of BODIPY that were used in this study (*N*-(4,4-difluoro-5,7-dimethyl-4-bora-3a,4a-diaza-*s*-indacene-3-yl)methyl)-iodo-acetamide (SBDY) and *N*-(4,4-difluoro-5,7-dimethyl-4-bora-3a,4a-diaza-*s*-indacene-3-propionyl)-*N*′-(iodoacethylene-diamine) (LBDY)) are shown in Fig. 1 *C*. Both are commercially available from Molecular Probes, (Eugene, OR). The SBDY and LBDY probes are covalently linked to a cysteine residue in a protein by replacing the I atom in the probe with the S atom of the cysteine residue. The Förster radius (R_0) was determined to be ~60 Å for different labeled single Cys mutants. A scatter in the R_0 values was observed that correlated with varying amounts of I-ions remaining from the labeling procedure. The reason for the scattering values is the overlap between the absorption spectra of the ions and BODIPY, which, depending on the ion concentration, will have a different influence on the calculated R_0 value. To avoid this complication, we have used $R_0 = 57 \pm 1$ Å [$\langle\kappa^2\rangle = 2/3$], which was previously obtained for various BODIPY derivatives in ethanol (Karolin et al., 1994). As compared to BODIPY, the absorption and fluorescent spectra of SBDY and LBDY are slightly red shifted by ~1 nm. For both derivatives, the maximum molar absorptivity in ethanol has been determined to be 80,000 M^{-1} cm^{-1} at 505 nm.

Construction and expression of PAI-1 Cys mutants

The construction of the single PAI-1 Cys mutants S344C and N329C, corresponding to the P3 and P18 residues of the reactive center loop (Carrell and Evans, 1992), has been described earlier (Strandberg et al., 1994; Fa et al., 1995). For the in vitro mutagenesis H185C of PAI-1, the oligomer 5′-CTGAGGTCGTGGTGTGCGGCGGAGAAGGTG-3′ was used, where the nucleotides deviating from the wild-type sequence are underlined. The double mutants S344C-N329C and S344C-H185C were constructed by using the same strategy, and by using c-DNA of the single mutants as the template. The expression and purification of the PAI-1 mutants were performed as described elsewhere (Fa et al., 1995).

Labeling of PAI-1 Cys-mutants with BODIPY derivatives

Active PAI-1 Cys-mutants (5 μM) dissolved in PBST (50 mM sodium phosphate buffer, pH 7.4, containing 150 mM NaCl and 0.01% Tween-80), were labeled by the addition of SBDY (or LBDY) dissolved in 100% dimethyl sulfoxide. In the reaction mixture, the final concentrations of dimethyl sulfoxide and the reactive label were 10% (by volume) and 250 μM, respectively. The reaction was performed in the dark for 2 days at room temperature. Subsequently, excess of probes was removed by gel filtration on a NAP-25 column (Pharmacia), equilibrated with PBST buffer. The labeled inhibitor was then incubated at 37°C overnight to ensure full conversion to the conformationally different latent form (Mottonen et al., 1992). The incorporation efficiency was calculated from the absorption spectra of the probes and PAI-1 by using molar absorptivities of ϵ_{probes} ($\lambda_{\max}$ = 505 nm) = 80,000 M^{-1} cm^{-1} and $\epsilon_{\text{latent PAI-1}}$ ($\lambda_{\max}$ = 280 nm) = 28,667 M^{-1} cm^{-1}. The efficiencies of labeling were 90–100% for the double mutants and 50–90% for the single mutants. The inhibitory activities of all PAI-1 Cys mutants (both nonlabeled and labeled) were similar to that obtained for the wild-type inhibitor (Strandberg et al., 1994; Fa et al., 1995; Aleshkov et al., 1996).

Fluorescence measurements

To eliminate the influence of protein rotation on the fluorescence timescale, all samples contained 50% (by volume) of glycerol (quartz glass distilled; BDH). The influence of glycerol on the activity of PAI-1 is negligible (Fa et al., 1995). For each set of labeled PAI-1 mutants (that is, double as well as the corresponding single mutants), two independent preparations and fluorescence experiments were performed. The temperature of the samples was kept at 277 ± 0.5 K. To avoid reabsorption, the maximum absorbance was kept below 0.08. The fluorescence spectra and steady-state anisotropies were determined on a SPEX fluorolog 112 instrument equipped with Glan-Thompson polarizers. The excitation and emission bandwidths were set to 5.6 nm and 2.8 nm, respectively. The mean value of the steady-state emission anisotropy (r_s, excited at 500 nm) was calculated by integration of

$$r_s(\lambda) = \frac{F_{VV}(\lambda) - g(\lambda)F_{VH}(\lambda)}{F_{VV}(\lambda) + 2g(\lambda)F_{VH}(\lambda)}$$

over the region 520–560 nm. Here F denotes the fluorescence intensity, and the first and second subscripts indicate the settings (vertical (V) or horizontal (H)) of the excitation and emission polarizers, respectively. The correction factor $g(\lambda) = F_{HV}(\lambda)/F_{HH}(\lambda)$ compensates for different transmission efficiency of vertically and horizontally polarized light, and it was determined from measurements on BODIPY dissolved in ethanol.

The single photon counting experiments were performed on a PRA 3000 system (Photophysical Research Associates, London, ON, Canada). The excitation source was a thyratron-gated flash lamp (PRA; model 510C) filled with deuterium gas and operated at ~30 kHz. The excitation and emission wavelengths were selected by interference filters (Omega/Saven AB, Stockholm, Sweden) centered at 500 nm (half-bandwidth (HBW) = 12.1 nm) and 550 nm (HBW = 40 nm), respectively. The instrument response function was determined with a light-scattering solution (Ludox).

The time-resolved fluorescence anisotropy was determined by repeatedly collecting fluorescence decay curves with the excitation polarizer alternating between the parallel [$F_{VV}(t)$] and horizontal [$F_{HV}(t)$] positions, and the emission polarizer was set in the vertical position. The total number of counts, F_{VV}^{tot} and F_{HV}^{tot} for the different polariser settings $F_{VV}(t)$ and $F_{HV}(t)$, were determined by integration of the intensity over the whole range of the decay curve. From the measured decay curves, a sum curve

$$s(t) = F_{VV}(t) + 2KF_{HV}(t)$$

and a difference curve

$$d(t) = F_{VV}(t) - KF_{HV}(t)$$

were constructed. The scaling factor K was calculated from

$$K = (1 - r_s)(1 + 2r_s)^{-1}F_{VV}^{tot}(F_{HV}^{tot})^{-1}$$

The maximum number of counts in the maximum of the $d(t)$ curves was always ~20,000 counts.

Data analysis

The experimental difference [$D(t)$] and sum [$S(t)$] curves were constructed according to

$$D(t) = \int_0^t E(t - x)r(x)w(x)dx$$

and

$$S(t) = \int_0^t E(t - x)w(x)dx$$

where $E(t - x)$, $r(t)$, and $w(t)$ denote the instrumental response function, the fluorescence anisotropy, and photophysics decays, respectively. The photophysics obtained by deconvolution of $S(t)$ was used for deconvoluting $r(t)$ from $D(t)$. For reconvolutions, a nonlinear least-squares analysis was used, based on the Levenberg-Marquardt algorithm. The fitting range over $d(t)$ was ~45 ns, starting from the maximum of the response function. To ensure that the fitting is reasonable, the steady-state fluorescence anisotropy was calculated from $r(t)$ and $w(t)$ and compared with the experimental value. The quality of the fit was judged by the global χ^2 value and the χ^2 values calculated for each set of data, as well as by the residual graphs. The calculations were performed on a Silicon Graphics, IRIS INDIGO workstation equipped with a MIPS R4000 processor.

Synthetic single-photon counting data

For testing models that describe fluorescence decays, it is important to know how well the decay parameters can be recovered in the deconvolution process. For this purpose, it is valuable to generate synthetic fluorescence data that mimic a real experiment, and for which all model parameters are known. From the reanalysis of such data and by comparing known and recovered parameters, one can judge the stability of the model under investigation. In this work, data were generated by a Monte Carlo convolution method (Fahmida et al., 1991), which automatically provides the relevant statistics of single-photon-counting experiments, i.e., the Poisson statistics. A brief outline of this method in the context of fluorescence depolarization experiments is given below.

The mathematical expression for the anisotropy, $r(t)$, describing energy transfer in bichromophoric molecules, depends on a set of parameters.

Knowing these parameters, the polarized fluorescence decays $I_{VV}(t)$ and $I_{HV}(t)$ are constructed according to

$$I_{VV}(t) = [1 + 2r(t)]w(t)$$

$$I_{HV}(t) = [1 - r(t)]w(t)$$

The fluorescence decays, $F_{VV}(t)$ and $F_{HV}(t)$, obtained from experiments, are convolutions of the true decay functions $I_{VV}(t)$ and $I_{HV}(t)$ with the normalized instrumental response function $\{E(t)\}$:

$$F_{VV}(t) = \int_0^t E(t - \tau)I_{VV}(\tau)\mathrm{d}\tau$$

$$F_{HV}(t) = \int_0^t E(t - \tau)I_{HV}(\tau)\mathrm{d}\tau$$

In the Monte Carlo convolution method, two random numbers, X_E and X_I, are generated to follow the density functions $E(t)$ and $I_{AV}(t)$ (A = V or H), respectively. Two kinds of random number generators were used, one for generating a uniform distribution of numbers between 0 and 1, and a second one for generating discrete random numbers of a specific distribution. We used the uniform pseudo-random number generator of Marsaglia (Marsaglia and Zaman, 1987) and the alias method (Kronmal and Peterson, 1979) to convert the uniform distribution into discrete random numbers. The sum of X_E and X_I represents the time for one emission event. By generating several emission events, a histogram can be constructed that is the discrete function $F_{AV}(t)$ given by the convolution integral above. The instrumental response function, $E(t)$, was taken to be a Gaussian distribution with the same full width at half-maximum as that of the experimental response function, that is, ~1.5–2 ns. The time resolution was 0.16 ns/channel. To minimize the round-off errors inherent in this method, each channel was split into 32 subchannels that were summed up after the random convolution. The number of counts in each decay was the same as in real experiments. From the generated decay curves, the steady-state fluorescence anisotropy was calculated from

$$r_s = \frac{\int_0^\infty r(t)w(t)\mathrm{d}t}{\int_0^\infty w(t)\mathrm{d}t}$$

The synthetic decay data were then analyzed by using the procedure described above (see Data Analysis).

RESULTS AND DISCUSSION

Model

The time-resolved fluorescence anisotropy, $r(t)$, is an orientational correlation function that correlates the orientation of the excited molecules (given by Eulerian angles Ω_0 and Ω) at the times of excitation ($t = 0$) and emission ($t = t$). The rotation of an excited molecule and the excitation energy migration contribute to ($t = 0$). We assume that the orientational correlation functions $\{r_j(t)\}$ and the excitation probability $\{p(t)\}$ of the two d molecules can be separated, and that the fluorescence anisotropy can be written as

$$r(t) = \frac{1}{2}\{r_1(t) + r_2(t)\}p(t) + \frac{1}{2}\{r_{12}(t) + r_{21}(t)\}\{1 - p(t)\} \quad (1)$$

Here $r_{ij}(t)$ denotes contributions due to energy migration from the initially excited d_i molecule to its neighbor d_j. Note that the excitation probability is $p(t)$ for any donor being the initially excited one. Recently, the Liouville equation of energy transfer between a pair of coupled dd molecules undergoing Brownian rotational motions was studied (Fedchenia and Westlund, 1994). It was concluded that cross-correlation between $r_j(t)$ and $p(t)$ is negligible, which supports the use of this assumption in Eq. 1.

For extracting molecular information from Eq. 1, expressions for $r_j(t)$, $r_{ij}(t)$, and $p(t)$ are needed. The rotational correlation functions $r_j(t)$ are given by

$$r_j(t) = \frac{2}{5}\sum_{m=-2}^{2}\langle D^{(2)}_{m0}(\Omega^0_{LM_j})D^{(2)}_{-m0}(\Omega_{LM_j})\rangle(-1)^m \quad (2)$$

The brackets $\langle \ldots \rangle$ denote orientational averages over the ensemble of d molecules, and $D^{(2)}_{m0}(\Omega_{LMj})$ are second-rank Wigner rotational matrices (Brink and Satchler, 1993). The subscripts LM_j indicate the transformation (see Fig. 2) from the laboratory (L) to the molecular (M_j) frame. The corresponding expression for $r_{ij}(t)$ reads

$$r_{ij}(t) = \frac{2}{5}\sum_{m=-2}^{2}\langle D^{(2)}_{m0}(\Omega^0_{LM_i})D^{(2)}_{-m0}(\Omega_{LM_j})\rangle(-1)^m \quad (3)$$

The reorientational motions of the d molecules attached to a macromolecule, like a protein, are of global and local nature. The local mobility is schematically illustrated in Fig. 2, where each d molecule can undergo anisotropic rotations with respect to its local frame D_i. Because intramolecular dd interactions depend on the distance between the donors, it is convenient to introduce another frame (R) fixed in the macromolecule and connecting the D_i frames. The local orientational distribution of each fluorophore is anisotropic, and it is denoted by $f_i(\Omega_{D_iM_i})$. The global motion of the macromolecule is assumed to be negligible on the time scale of fluorescence, and the orientational distribution $F(\Omega_{LR})$ is isotropic. The evaluation of Eqs. 2 and 3 involves the orientational transformations of $\Omega_{LR} \rightarrow \Omega_{RD_i} \rightarrow \Omega_{D_iM_i}$, and the averaging over the corresponding orientational distribution functions, $F(\Omega_{LR})$, $h_i(\Omega_{RD_i})$, and $f_i(\Omega_{D_iM_i})$. For a uniaxial distribution $f_i(\Omega_{D_iM_i})$ about the z axis of the D_i frames, and $h_i(\Omega_{RD_i})$ that is discrete, Eq. 2 can be written

$$\langle D^{(2)}_{m0}(\Omega^0_{D_iM_i})D^{(2)}_{-m0}(\Omega_{D_iM_i})\rangle = \iint f_i(\Omega^0_{D_iM_i})D^{(2)}_{m0}(\Omega^0_{D_iM_i})g_i(\Omega^0_{D_iM_i}/\Omega_{D_iM_i}, t) \times D^{(2)}_{-m0}(\Omega_{D_iM_i})\mathrm{d}\Omega^0_{D_iM_i}\,\mathrm{d}\Omega_{D_iM_i} \quad (4)$$

In Eq. 4, $g_i(\Omega^0_{D_iM_i}/\Omega_{D_iM_i}, t)$ is the probability density for the orientation $\Omega_{D_iM_i}$ at time t, given the initial orientation of $\Omega^0_{D_i}M_i$.

To treat the reorientation of the *d* molecules, we used the simple strong collision model, $g_i(\Omega^0_{D_iM_i}/\Omega_{D_iM_i}, t) = \{\delta(\Omega_{M_iD_i} - \Omega^0_{M_iD_i}) - f(\Omega_{M_iD_i})\}\gamma_i(t) + f(\Omega_{M_iD_i})$. Here $\gamma_i(t)$

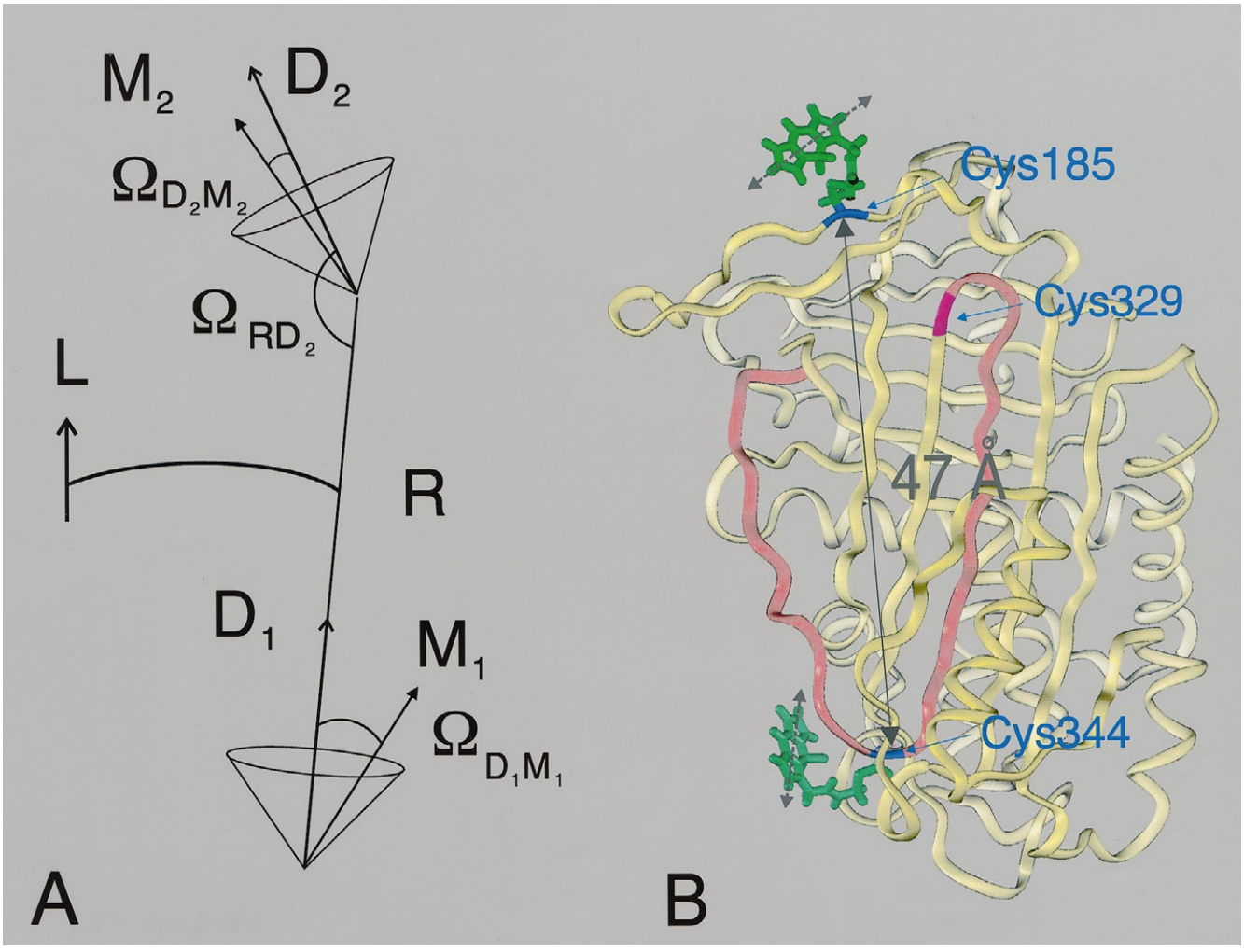

FIGURE 2 (*A*) The scheme illustrates the different frames involved in describing energy transfer within a bichromophoric molecule. Here R denotes a molecule fixed frame. The donor molecules (denoted as numbers 1 and 2) are uniaxially oriented about the *z* axes of the D_1 and D_2 frames. Ω denotes the Euler angles and provides the orientational transformations between the laboratory (L), R, D_i, and molecular (M_i) frames. The arrows of M_1 and M_2 indicate the electronic transition dipole moment. (*B*) The figure shows the ribbon model of latent PAI-1 double mutant H185C-S344C with the fluorescent probe (*in green*), attached to the cysteine residues. The model was created with the Insight II program (Biosym Technologies, San Diego, CA). The distance of 47 Å indicated is that between the C_α atoms of Cys^{185} and Cys^{344}. The apolar vectors show the polarization of the electronic transition dipole moment.

is an exponential function or a sum of exponential functions. Hence Eqs. 2 and 4 can be written as

$$r_i(t) = \frac{2}{5}\{(1 - \rho_i^\infty)\gamma_i(t) + \rho_i^\infty\} \tag{5}$$

where $\rho_i^\infty = \langle D_{00}^{(2)}(\Omega_{M_iD_i})\rangle^2$ and $\langle D_{00}^{(2)}(\Omega_{M_iD_i})\rangle$ is a second-rank-order parameter that ranges between $-1/2$ and 1.

By averaging the correlation function in Eq. 3 over $F(\Omega_{LR}) = 1/8\pi^2$, one obtains

$$r_{ij}(t) = \frac{2}{5}\sum_{m,q,q'}\langle D_{mq}^{(2)}(\Omega_{RD_i})D_{-mq'}^{(2)}(\Omega_{RD_j})D_{q0}^{(2)}(\Omega_{D_iM_i}^0)D_{q'0}^{(2)}(\Omega_{D_jM_j})\rangle \cdot(-1)^m \tag{6}$$

The modeling of this contribution to the fluorescence anisotropy is subtle. The term $r_{ij}(t)$ originates from secondary excitation caused by energy migration from the initially excited d_i molecule to its neighbor d_j. For sufficiently long times, i.e., $t \geq t_\infty$, there is no orientational correlation between the initially and the secondary excited molecules. Therefore, $r_{ij}(t)$ will reach its residual value of

$$r_{ij}(t_\infty) = \frac{2}{5}D_{00}^{(2)}(\delta)\langle D_{00}^{(2)}(\Omega_{D_iM_i})\rangle\langle D_{00}^{(2)}(\Omega_{D_jM_j})\rangle \equiv \frac{2}{5}\rho_{ij}^\infty \tag{7}$$

where δ is the angle between the symmetry axes of the uniaxial distributions (D_1 and D_2 in Fig. 2). The probability of secondary excitation will depend on angular dependence of the mechanism for energy transfer. For weak interaction according to Förster (1948), this is given by the angular part of dipole-dipole coupling, which is denoted by $\tilde{\kappa}^2(\Omega_{D_iM_i}, \Omega_{D_jM_j}, \Omega_{RD_i}, \Omega_{RD_j})$ (see Appendix). In the static limit, and

initially, Eq. 6 is given by

$$r_{ij}(0) = \frac{2}{5}\sum_{m,q,q'}\int_{\Omega_{RD_i}}\int_{\Omega^0_{D_iM_i}}\int_{\Omega_{RD_j}}\int_{\Omega_{D_jM_j}} \cdot h_i(\Omega_{RD_i})D^{(2)}_{mq}(\Omega_{RD_i})h_j(\Omega_{RD_j})D^{(2)}_{-mq'}(\Omega_{RD_j})f_i(\Omega^0_{D_iM_i}) \times D^{(2)}_{q0}(\Omega^0_{D_iM_i})\tilde{\kappa}^2(\Omega_{RD_i}, \Omega^0_{D_iM_i}, \Omega_{RD_j}, \Omega_{D_jM_j}) \cdot D^{(2)}_{q'0}(\Omega_{D_jM_j})(-1)^m\, d\Omega_{RD_i}\, d\Omega^0_{D_iM_i}\, d\Omega_{RD_j}\, d\Omega_{D_jM_j} \equiv \frac{2}{5}\rho^0_{ij} \quad (8)$$

Equation 8 yields the maximum contribution to $r(t)$ from secondary excited donor molecules. In particular, for isotropically oriented donor molecules, one obtains $r_{ij}(0) = 2/125$, which was also previously obtained by Baumann and Fayer (1986). In this case and regarding experimental accuracy, this contribution to $r(t)$ is negligible. However, for locally anisotropic orientational distributions, the magnitude of $r_{ij}(t)$ can become comparable to $r(t)$. To model the time dependence contribution from secondary excited donors, we assume

$$r_{ij}(t) = \frac{2}{5}\{(\rho^0_{ij} - \rho^\infty_{ij})\gamma_i(t) + \rho^\infty_{ij}\} \quad (9)$$

The excitation probability of the initially excited donor [$p(t)$] within a dd pair is, in the dynamic and slow limits, easily obtained from the master equation, which is given by

$$p(t) = \frac{1}{2}\{1 + \exp(-2\omega t)\} \quad (10a)$$

$$\omega = \frac{3}{2}\langle\kappa^2\rangle\left(\frac{R_0}{R}\right)^6\tau^{-1} \quad (10b)$$

where the fluorescence lifetime, the Förster radius, and the intramolecular distance are denoted by τ, R_0, and R, respectively. The average angular dependence of dipole-dipole coupling, $\langle\kappa^2\rangle$, is further specified in the Appendix. In the dynamic limit, the transfer rate (ω) is much slower than the rates of donor reorientations, and the average value of $\langle\kappa^2\rangle$ can be expressed in terms of second-rank-order parameters according to

$$\langle\kappa^2\rangle = \frac{2}{3} + \frac{2}{3}D^{(2)}_{00}(\delta)\langle D^{(2)}_{00}(\Omega_{D_iM_i})\rangle\langle D^{(2)}_{00}(\Omega_{D_jM_j})\rangle + \frac{2}{3}\{D^{(2)}_{00}(\Omega_{RD_i})\langle D^{(2)}_{00}(\Omega_{D_iM_i})\rangle + D^{(2)}_{00}(\Omega_{RD_j})\langle D^{(2)}_{00}(\Omega_{D_jM_j})\rangle\} + \frac{4}{3}D^{(2)}_{00}(\Omega_{RD_i})D^{(2)}_{00}(\Omega_{RD_j})\langle D^{(2)}_{00}(\Omega_{D_iM_i})\rangle\langle D^{(2)}_{00}(\Omega_{D_jM_j})\rangle - 6\sin\beta_{RD_i}\cos\beta_{RD_j} \times \sin\beta_{RD_i}\cos\beta_{RD_j}\cos\alpha_{RD_ji}\langle D^{(2)}_{00}(\Omega_{D_iM_i})\rangle \cdot \langle D^{(2)}_{00}(\Omega_{D_jM_j})\rangle \quad (11)$$

By using Eqs. 5, 7, 9, and 10 and the assumptions given above, it is possible to derive an explicit expression for Eq. 1. To calculate $\langle\kappa^2\rangle$ from Eq. 11, it is necessary to know the order parameters of each donor with respect to its local symmetry axis, the angles between the latter axes and the intramolecular R vector, and the mutual angle (δ) between the local symmetry axes. It is possible, however, to obtain the order parameter of each d molecule from fluorescence anisotropy experiments (see Eq. 5). Then, by using these order parameters, δ could be calculated from the residual anisotropy of the dd system, as can be seen by inserting Eqs. 5, 7, and 10 in Eq. 1 at the times of $t \geq t_\infty$ and $t \gg 1/\omega$. For calculating $\langle\kappa^2\rangle$, one still needs three more angles, namely, the angle between the local symmetry axes and the R vector, as well as their (D_1, D_2) mutual azimutal rotation angle about R. To circumvent this difficulty, we approximate one of the local symmetry axes to be effectively along R. The local axis for which the order parameter takes the smallest value is chosen. This approximation gives

$$\langle\kappa^2\rangle = \frac{2}{3} + \frac{2}{3}\langle D^{(2)}_{00}(\Omega_{D_iM_i})\rangle + \frac{2}{3}\langle D^{(2)}_{00}(\Omega_{D_jM_j})\rangle D^{(2)}_{00}(\delta) + 2\langle D^{(2)}_{00}(\Omega_{D_iM_i})\rangle\langle D^{(2)}_{00}(\Omega_{D_jM_j})\rangle D^{(2)}_{00}(\delta) \quad (12)$$

Hence all parameters in Eq. 12 are available from the residual anisotropies obtained for each d molecule and the dd pair.

To examine further the influence of reorientation on energy migration within dd pairs, as well as its influence on the fluorescence anisotropy, the stochastic master equation has recently been derived and formally solved, as it is derived from the stochastic Liouville equation (Johansson et al., 1996b). In a forthcoming paper, the model presented here is examined by means of the stochastic Liouville theory and simulation methods.

Choice of d molecules

In the model presented above, it is assumed that the photophysics of each d molecule within a pair is the same. In practice, however, the photophysics of many fluorescent probes are more or less sensitive to the polarity, pH, and presence of quenching molecules. These properties may, of course, differ considerably between different regions of a protein. Consequently, the choice of fluorescent label is important. We have found (Karolin et al., 1994) that derivatives of the recently developed fluorophore, 4,4-difluoro-4-borata-3a-azonia-4a-aza-*s*-indacence (BODIPY), meet this requirement, as well as other important criteria, very well. The fluorescence lifetime of the probe is ~5.5 ns, and it is independent of pH and changes very little with solvent polarity. However, both Trp and Tyr may quench BODIPY with quenching constants of ~15 M^{-1}. Therefore, when

labeling a protein molecule at different positions, it is necessary to examine the photophysics decay for each choice of site.

Mono- and bichromophoric proteins

Substitution mutants of PAI-1, containing one or two cysteine residues, were constructed by using site-specific mutagenesis, as described in Materials and Methods. We have studied the single mutants S344C, N329C, and H185C and the double mutants S344C-N329C and S344C-H185C (see Fig. 1 *B*). The long and short linker forms of BODIPY, denoted by LBDY and SBDY, respectively, were covalently bound to the cysteine residues of the mutants. The degree of labeling of the double mutants was always better than 90%. To eliminate the influence of rotation of the protein molecules on the fluorescence anisotropy, all solutions contained 50% glycerol (by volume). The fluorescence decay of all mutants is found to be nearly monoexponential, with a dominating lifetime of ~5.3 ns (see Table 1).

The fluorophore-labeled PAI-1 mutants were characterised in terms of the inhibitory activity against target proteases (plasminogen activator). The inhibitory activity of the labeled mutants was found to be similar to that of the wild-type inhibitor. This suggests that the mutants maintain the tertiary structure of the wild type. The model of latent PAI-1 with the fluorescent probe molecules attached at positions 344 and 185 (Fig. 2) is based on the crystal structure of latent PAI-1 (Mottonen et al., 1992). Note that Fig. 2 shows only the backbone of latent PAI-1. The SBDYs are inserted to illustrate their possible location. Therefore, in the absence of amino acid side chains, it appears that the probes may have a high degree of orientational freedom (i.e., low order parameters).

Intramolecular order and reorientation

The time-resolved fluorescence anisotropy of the labeled PAI-1 single mutants gives information about the local rotational rate of the fluorescent group, as well as about its local orientational restriction, or order (ρ_i^∞; see Eq. 5). The decay of $r_i(t)$ can be obtained from the difference curve by fitting with one rotational correlation time (ϕ_i) and a static term (ρ_i^∞) according to Eq. 5 (Fig. 3). The rotational correlation time varies between ~6 and 12 ns for BODIPY in the different positions of PAI-1, as shown in Table 2. Note that the rotational correlation times are significantly different for SBDY and LBDY in H185C, whereas within experimental accuracy they are similar for the S344C mutants. This is compatible with a different, although likely small, localization of the BODIPY group in LBDY and SBDY probes. Because the residual anisotropies are rather high for the single mutants (i.e., $r_i(t_\infty) > 0.15$), the order parameters must take positive values, i.e., $\langle D_{00}^{(2)}(\Omega)\rangle > 0.5$. Furthermore, the large values of the order parameters (see Table 2) mean that the local orientational restrictions of the BODIPY moieties are high. The initial anisotropy values [$r(0)$] were always found to be smaller than the limiting anisotropy value of $r_0 = 0.37$ (Karolin et al., 1994). This strongly suggests a small influence from rapid motions of the BODIPY moiety, such as librational or rotational motions (10^{-12} to 10^{-11} s), which are beyond the time resolution of the experimental equipment.

Intramolecular distances

To analyze the $r(t)$ data obtained for the labeled double mutants of PAI-1, we assume that the rates and restrictions of local motions are very similar to those of the corresponding single mutants. This assumption is supported by the fact that the probes are localized far away from each other in the protein structure, and that formation of the Cys mutant and its labeling do not have any significant influence on the inhibitory activity. Under these circumstances, the strategy of global analysis (Knutson et al., 1983; Löfroth, 1985) could be applied. In this application, it means that the model presented above (i.e., Eqs. 1, 5, 9, and 10) is simultaneously fitted to the depolarization data obtained for the two single

TABLE 1 Different single and double Cys-mutants of latent PAI-1

Probe	Mutant	τ_1 (ns)	τ_2 (ns)	f_2	$\langle\tau\rangle$ (ns)	DW	χ^2
SBDY	S344C	5.3 ± 0.1			5.3	1.67	1.15
	H185C	5.3 ± 0.1	6.2 ± 0.4	0.22	5.5	2.14	1.06
	S344C-H185	5.4 ± 0.1			5.3	1.81	1.07
	N329C	5.4 ± 0.1			5.4	2.03	1.07
	S344C-N329C	5.4 ± 0.1	2.2 ± 0.9	0.06	5.3	1.92	1.13
LBDY	S344C	5.6 ± 0.1			5.6	2.07	0.99
	H185C	5.6 ± 0.1			5.6	1.95	1.13
	S344C-H185C	5.6 ± 0.1			5.6	1.61	1.15
	N329C	5.5 ± 0.1			5.5	1.75	1.10
	S344C-N329C	5.6 ± 0.1	2.4 ± 0.9	0.05	5.5	1.97	0.98

The double mutants have position S344C in common. The mutants have been labeled with the fluorophore BODIPY, which is connected to the protein with either a short linker (SBDY) or a long linker (LBDY). The fluorescence lifetimes (τ_1) obtained by fitting a sum of two exponential functions [$a_1 \exp(-t/\tau_1) + a_2 \exp(-t/\tau_2)$] to the fluorescence decay and the average lifetime $\langle\tau\rangle$ are given for LBDY and SBDY derivatives of BODIPY in various systems of latent PAI-1. The average lifetime was calculated from $\langle\tau\rangle = (a_1\tau_1^2 + a_2\tau_2^2)/(a_1\tau_1 + a_2\tau_2)$. The fraction of fluorescence intensity caused by lifetime component number 2 are denoted by f_2 and are calculated from $f_2 = a_2\tau_2/(a_1\tau_1 + a_2\tau_2)$. For judging on the quality of fitting, a biexponential fluorescence decay, the Durbin-Watson (DW), and the χ^2 parameters are presented.

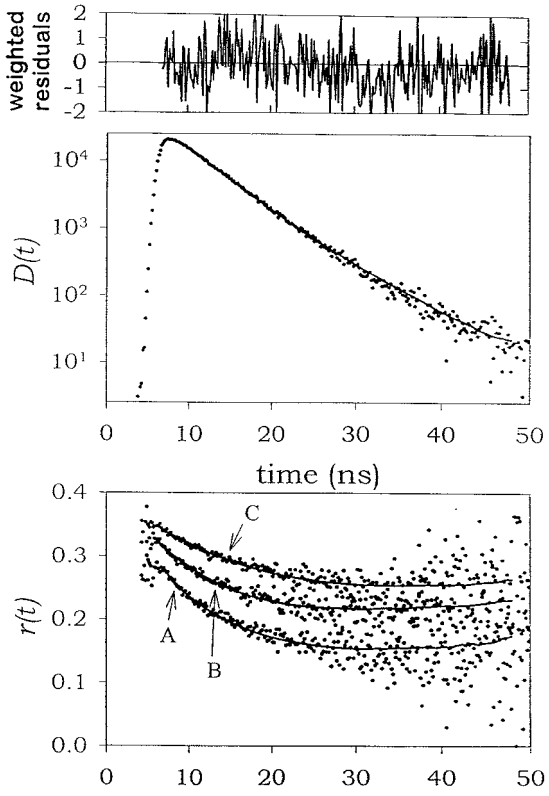

FIGURE 3 Example of decay curves for the latent PAI-1 S344C-H185C system labeled with SBDY. The upper graph shows the fitted difference curve of the double mutant together with the weighted residuals. The lower graph shows the anisotropy decay for (*A*) S344C-H185C, (*B*) S344C, and (*C*) H185C. The $r(t)$ curves were constructed by dividing the $d(t)$ and $s(t)$ decay curves. Consequently, they do not represent the true shape of $r(t)$, because the response function has a half-width at full maximum of ~2 ns, and furthermore, it is tailing, which introduces a small apparent increase of $r(t)$ at long times.

mutants and the double mutant of PAI-1. For the PAI-1 mutants studied here, it proved sufficient to use one rotational correlation time (ϕ_i). Taken together, this gives the following equations for the fluorescence anisotropies:

$$r_i(t) = b_i \exp(-t/\phi_i) + r_0\langle D_{00}^{(2)}(\Omega_{D_iM_i})\rangle^2 \qquad i = 1, 2 \quad (13a)$$

$$r(t) = \frac{1}{4}\{r_1(t) + r_2(t)\}\{1 + \exp(-2\omega t)\} + \frac{1}{4}r_0(\{\rho_{12}^0 - \rho_{12}^\infty\}\{\exp(-t/\phi_1) + \exp(-t/\phi_2)\} + 2\rho_{12}^\infty)\{1 - \exp(-2\omega t)\} \quad (13b)$$

where fluorescence anisotropy decays $r_i(t)$ and $r(t)$ refer to the single mutants and double mutants, respectively. The coefficients b_i in Eq. 13a are fitting parameters that are related to the initial and the residual anisotropies according to $b_i = r_i(0) - r_0\langle D_{00}^{(2)}(\Omega_{D_iM_i})\rangle^2$. The $r_i(t)$ and $r(t)$ decays were obtained from the difference and sum curves (as described in Data Analysis). In Fig. 3, typical time-resolved fluorescence anisotropy data are displayed for the labeled single mutants S344C and H185C, as well as for the double mutant S344-H185C. The more rapid decay found for the double mutant, as compared to the single mutants, is compatible with energy migration. In the absence of energy migration, the $r(t)$ decay would be located as an average decay given by $[r_1(t) + r_2(t)]/2$. The analysis of one data set gives values on the rate of energy migration, as well as order parameters. By using these values and Eq. 10b, the intramolecular distance (R) can be calculated (see Table 2). The R values given in Table 2 are the arithmetic averages obtained for independent preparations and experiments for the different sets of PAI-1 mutants. For a comparison, the distances (R_c) between the two C_α atoms corresponding to mutated amino acid residues in the PAI-1 double mutant were determined from the crystal structure of the wild-type latent PAI-1 (Mottonen et al., 1992). The small differences in R values obtained for SBDY and LBDY indicate that the localization of the BODIPY groups is slightly different, which is quite reasonable, because the linkers are different. However, there is still good agreement between R and R_c for both SBDY and LBDY, indicating that the linker is adopting a rather nonextended conformation.

To examine the extension of the linkers, the average distance between the C_α atom of the cysteine residue and the center of mass of the chromophore was studied by means of Monte Carlo simulations. The conformation space, in vacuum, of the chromophore and the linker connected to a cysteine amino acid was sampled by using the MM2 force field (Allinger, 1977). In the simulations, only nonbonded interactions of the MM2 force field were considered, that is, the van der Waals and bond dipole interactions. With the exception of the peptide bonds, the bonds of the linker were allowed to rotate through a random angle. The algorithm of Metropolis (Metropolis et al., 1953) was used. The rotation angles were modified during the simulation, so that ~50% of the rotations were accepted. The distance between the C_α atom and the chromophore moiety of the probe was calculated. We found average distances of 9.4 and 5.8 Å between the center of mass of the chromophore and the C_α atom for the long and short linkers, respectively. The corresponding distances for the fully extended linkers are 16.5 and 11.0 Å. This indicates that the linkers tend to adopt a folded conformation. Qualitatively, this agrees with our experimental results.

Although the resolution of the DDEM method can be improved by using probes with shorter linkers and by tuning the Förster radius, it is important to note that the DDEM method cannot give an atomic resolution of protein structures. Still, the DDEM method can be a valuable tool for examining structural changes. Recently this was demonstrated in two reports focusing on the cleavage and the translocation of protein segments in PAI-1 (Aleshkov et al., 1996; Wilczynska et al., 1997).

TABLE 2 Different single and double Cys-mutants of latent PAI-1

Probe	Mutants	r_s	ϕ (ns)	$r(0)$	ρ^0	$r(t_\infty)$	$\langle D_{00}^{(2)}(\Omega_{DM})\rangle$	$\omega \times 10^{-9}$ s^{-1}	$\langle\kappa^2\rangle$	δ (°)	R (Å)	R_c (Å)
SBDY	S344C	0.273	7.0 ± 1.4	0.323		0.207	0.75					
	H185C	0.310	12.3 ± 2.5	0.344		0.231	0.79					
	S344C-H185C	0.226		0.333	0.60	0.128		1.6 ± 0.3	1.47	48	45.2 ± 1.2	46.8
	N329C	0.308	9.6 ± 2.4	0.323		0.241	0.81					
	S344C-N329C	0.211		0.342	0.44	0.148		2.1 ± 0.1	1.73	42	44.7 ± 0.2	37.8
LBDY	S344C	0.262	7.5 ± 1.0	0.329		0.174	0.68					
	H185C	0.247	6.8 ± 0.8	0.323		0.157	0.65					
	S344C-H185C	0.199		0.321	0.55	0.104		0.9 ± 0.1	1.52	42	50.8 ± 1.6	46.8
	N329C	0.274	7.0 ± 2	0.319		0.215	0.76					
	S344C-N329C	0.154		0.328	0.14	0.083		1.6 ± 0.2	1.09	55	43.2 ± 2	37.8

The double mutants have position S344C in common. The mutants have been labeled with the fluorophore BODIPY, which is connected to the protein with either a short linker (SBDY) or a long linker (LBDY). For each set of data, that is, for a labeled double mutant and its corresponding single mutants, the steady-state fluorescence anisotropy (r_S), rotational correlation time (ϕ), initial anisotropy ($r(0)$), residual anisotropy ($r(t_\infty)$), the rate of energy migration (ω), the order parameter ($\langle D_{00}^{(2)}(\Omega_{DM})\rangle$), $\langle\kappa^2\rangle$, δ^0 (see text), and the intramolecular distance (R) are presented. The errors indicated represent arithmetic mean values of two independent experiments. The errors of all parameters, except from ϕ, ω, and δ^0, are within ±4%. The distance (R) between the dd molecules is calculated (Eq. 10b) by using the average square angular dependence of dipole-dipole coupling ($\langle\kappa^2\rangle$), the angle between the symmetry axis of the orientational distributions (δ). The R values are compared with the distances (R_C) obtained by independent methods.

Analysis of synthetic data

Because the global analysis involves the determination of seven parameters, we have numerically tested the extent to which the quality of the data analysis depends on the rate of energy migration (ω). The three fluorescence anisotropy experiments and the parameters connected with them are ϕ_1, $\langle D_{00}^{(2)}(\Omega_{D_1M_1})\rangle$ from single mutant 1; ϕ_2, $\langle D_{00}^{(2)}(\Omega_{D_2M_2})\rangle$ from single mutant 2; and ω, $D_{00}^{(2)}(\delta)$, ρ^0 from the double mutant.

Synthetic data were generated by using the parameters obtained from the analysis of the short linker S344C-H185C system (see Table 2). Different sets of data were constructed for different ω values. The details of data generation given in Materials and Methods. The generated data were then analyzed by the same procedure as that used for the analysis of real data. Two different approaches were tested. In the first approach, all parameters were simultaneously fitted to the three sets of data. In the second approach, the single-mutant data were analyzed separately and the parameters determined were then used as fixed values in the analysis of the double mutant. Thus ω was the only variable. For the two approaches, a comparison between ω obtained from the data analysis and the value used for generating of the corresponding data is given in Fig. 4. For very slow rates, that is, $\omega \leq 10^8$ s^{-1}, the deviations become orders of magnitudes. This shows that the contribution of energy migration to the fluorescence decay has become too small to be detected. At rates of $\omega \approx 10^{11}$ s^{-1}, it is still possible to recover relevant results, although the rates correspond to a only fraction of the width of a time channel. For such fast rates it is of course necessary that time jitter and non-Poisson noise of the experimental equipment can be neglected. Hence, under optimum conditions for the system examined, it will be possible to recover migration rates in the range of 10^9 s$^{-1} < \omega < 10^{11}$ s^{-1}. These rates correspond to intramolecular distances (R) in the range of $0.4R_0 \leq R \leq 0.86R_0$ for the present set of data. Notice that for fast migration rates, the global target approach of analysis recovers slightly better values of ω. For slower migration rates, the correct value of ω is easier to extract if the rotational correlation times are fixed at the values obtained from a separate analysis of single mutant data.

Influence of partial labeling

When the intramolecular distance in a protein is determined by the model and methods described above, the double mutants must be labeled to nearly 100%. However, assume

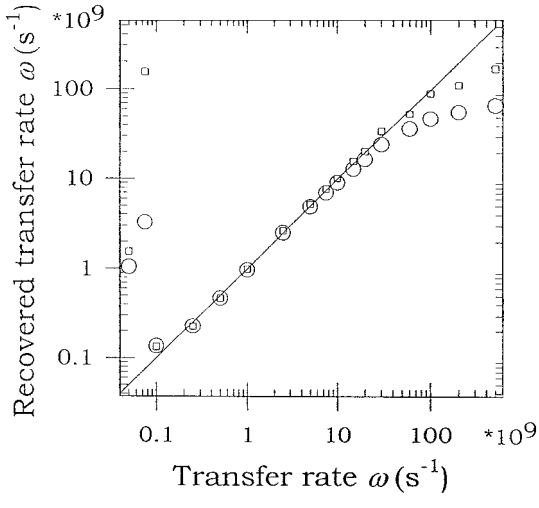

FIGURE 4 Recovered rates of energy migration (ω) as a function of known rates, obtained from the deconvolution of synthetic fluorescence anisotropy data. In one approach, all parameters were simultaneously fitted to the data of the two single mutants and the double mutant (□). In a second approach (○), the single-mutant data were analyzed separately, and the extracted parameters were used as fixed values in the analysis of the double mutant. The latter means that ω was the only variable. The order parameters and rotational correlation times were those experimentally determined for SBDY in H185C, S344C, and H185C-S344C of latent PAI-1 (see Table 2).

that the degree of labeling is lower, say 80% for the double mutant and 10% for each of the single mutants. It is then relevant to ask whether one could still analyze such data. Moreover, how does 90% instead of the expected 100% influence the calculated distance? To answer these questions, synthetic data were generated for the experimental parameters obtained from studies of the S344C, H185C, and S344C-H185C mutants. Data were generated for the double mutant containing 10%, 25%, and 40% mole fractions of the single mutants present. Provided the mole fractions are known and are less than 25%, the analysis of synthetic data is in excellent agreement with the expected values. Regarding the errors in the analysis of real data, one still obtains acceptable values of the distance that are within experimental error, even when the sample of double mutant contained a mole fraction of 40% single mutants, as could be seen from Table 3. Consequently, for the present set of data, 90% instead of 100% labeling would not influence the quality of extracted parameters. However, it is necessary to emphasize that this conclusion need not be valid for any other set of mutants. To be on the safe side, one should therefore test the reliability of parameters extracted from experiments by reanalyzing synthetic data. These findings suggest that it would be possible to analyze anisotropy data from partially labeled double mutants. This may increase the applicability of the method presented here, because it may very well be that only a partial labeling of the mutants could be achieved. We are currently examining such an extension of the present work.

CONCLUSIONS

It is possible to prepare fluorophore-labeled single and double mutants of the plasminogen activator inhibitor-1 (PAI-1) with minimum influence on the inhibitory activity. Two BODIPY derivatives (SBDY and LBDY) show very similar photophysics in different cysteine mutants of PAI-1. This is a prerequisite for using the fluorophore BODIPY as a dd pair for determining intramolecular distances.

The described method may be a powerful tool for determining conformation changes in proteins. For example, we have used this method to study molecular details in the inhibition of a target protease by PAI-1 (Wilczynska et al., 1997).

The model and methods presented for analyzing the fluorescence anisotropy data predict intramolecular distances that are in good agreement with independently determined values.

By analyzing synthetic data generated within the anisotropy model, one can assess the quality of the extracted parameters. Moreover, the effects on the extracted parameters that result from having mixtures of partially labeled double mutants can be investigated.

TABLE 3 Analysis of synthetic fluorescence data for different mixtures of double mutants (S344C-H185C) with labeled single mutants (S344C, H185C) of PAI-1.

f (%)	$\omega \times 10^{-9}$ s^{-1}	ρ^0	δ (°)	$\langle\kappa^2\rangle$	R (Å)
0	1.6	0.60	48	1.47	45.4
10	1.6	0.60	48	1.47	45.3
25	1.7	0.60	48	1.46	45.0
40	2.3	0.60	48	1.45	42.8
0	1.6	0.60	48	1.47	45.2

The fraction (f) of the two single mutants is taken to be the same, and otherwise the parameters obtained from the analysis of real data (see Table 2 for the short (SBDY) linker BODIPY) were used to generate synthetic data. The last row is presented for a comparison of the experimental results.

APPENDIX: THE ANGULAR PART OF DIPOLE-DIPOLE COUPLING

The angular part of dipole-dipole coupling (κ) can be written as (Johansson et al., 1996b)

$$\kappa = -\sqrt{30}\sum_{m=-1}^{1}\begin{pmatrix}1 & 1 & 2\\ m & -m & 0\end{pmatrix}D^{(2)}_{-m0}(\Omega_{RM_1})D^{(2)}_{m0}(\Omega_{RM_2}) \tag{A1}$$

where the Euler angles refer to transformations from the R frame to the molecular frames M_1 and M_2 (see Fig. 2). Each d molecule undergoes rotational motions ($\Omega_{D_iM_i}$) with respect to the local frame D_i, which has fixed orientation angles Ω_{D_iR} relative to the R frame. For rotational transformations where Ω_{RM_j} is replaced by $\Omega_{D_jM_j}$ and $\Omega_{D_jR_j}$, it is convenient to use the closure relation (Brink and Satchler, 1993)

$$D^{(J)}_{mp}(\Omega_{RM_j}) = \sum_n D^{(J)}_{mn}(\Omega_{RD_j})D^{(J)}_{np}(\Omega_{D_jM_j}) \tag{A2}$$

The relevant angular dependence for the rate of energy transfer is given by the square of κ as follows:

$$\begin{aligned}\kappa^2 = 30\sum_{m,m'}&\begin{pmatrix}1 & 1 & 2\\ m & -m & 0\end{pmatrix}\begin{pmatrix}1 & 1 & 2\\ m' & -m' & 0\end{pmatrix}\sum_{C,C'}(2C+1)\\ &\cdot(2C'+1)\begin{pmatrix}1 & 1 & 2\\ m' & -m' & 0\end{pmatrix}\begin{pmatrix}1 & 1 & 2\\ m' & -m' & 0\end{pmatrix}\\ &\cdot\begin{pmatrix}1 & 1 & C\\ -m & -m' & m+m'\end{pmatrix}\begin{pmatrix}1 & 1 & C'\\ m & m' & -m-m'\end{pmatrix}\\ &\times D^{(C)}_{m'm',0}(\Omega_{RM_1})D^{(C)}_{-m-m',0}(\Omega_{RM_2})\end{aligned} \tag{A3}$$

To calculate the contribution to the fluorescence anisotropy from secondary excited molecules, the probability function $\tilde{\kappa}^2(\Omega_{D_iM_i}, \Omega_{D_jM_j}, \Omega_{RD_i}, \Omega_{RD_j})$ appears in Eqs. 6 and 8. This probability is given by a normalization of Eq. A3, and by using Eq. A2, according to

$$\tilde{\kappa}^2(\Omega_{D_iM_i}, \Omega_{D_jM_j}, \Omega_{RD_i}, \Omega_{RD_j}) = \frac{\kappa^2(\Omega_{D_iM_i}, \Omega_{D_jM_j}, \Omega_{RD_i}, \Omega_{RD_j})}{\langle\kappa^2(\Omega_{D_iM_i}, \Omega_{D_jM_j}, \Omega_{RD_i}, \Omega_{RD_j})\rangle} \tag{A4}$$

We are grateful to Dr. B. Kalman at Linköping University for help in developing the deconvolution software.

This work was supported by the Swedish Natural Research Council (NFR K-AA/KU 08676-308 and NFR B-AA/BU 08473-311).

REFERENCES

Aleshkov, S., M. Fa, J. Karolin, L. Strandberg, L. B.-Å. Johansson, and T. Ny. 1996. Biochemical and biophysical studies of reactive centre cleaved plasminogen activator inhibitor type 1. The distance between P3 and P1′ determined by donor-donor fluorescence energy transfer. *J. Biol. Chem.* 271:21231–21238.

Allinger, N. L. 1977. Conformational analysis. 130. MM2. A hydrocarbon force field utilizing V_1 and V_2 torsional terms. *J. Am. Chem. Soc.* 99:8127–8132.

Bastiaens, P. I. H., S. G. Mayhew, E. M. O'Nualláin, A. van Hoek, and A. J. W. G. Visser. 1991. Energy transfer between the flavin chromphores of electron-transferring flavoproteins from *Megasphaera elsdenii* as inferred from time-resolved red-redge and blue-edge flourescence spectroscopy. *J. Fluorescence.* 1:95–103.

Baumann, J., and M. D. Fayer. 1986. Excitation transfer in disordered two-dimensional systems: effects of spatial geometry on time-resolved observables. *J. Chem. Phys.* 85:4087–4106.

Berberan-Santos, M. N., and B. Valeur. 1991. Fluorescence depolarization by electronic energy transfer in donor-acceptor pairs of like and unlike chromophores. *J. Chem. Phys.* 95:8048–8055.

Brink, D. M., and G. R. Satchler. 1993. Angular Momentum, 3rd Ed. Clarendon Press, Oxford.

Carrell, R. W., and D. L. I. Evans. 1992. Serpins: mobile conformations in family of protease inhibitors. *Curr. Opin. Struct. Biol.* 2:438–446.

Fa, M., J. Karolin, S. Aleshkov, L. Strandberg, L. B.-Å. Johansson, and T. Ny. 1995. Time-resolved polarized fluorescence spectroscopy studies of plasminogen activator inhibitor type 1: conformational changes of the reactive centre upon interactions with target proteases, vitronectin and heparin. *Biochemistry.* 24:13833–13840.

Fahmida, N. C., S. K. Zbigniew, and M. D. Barkley. 1991. Monte Carlo convolution method for simulation and analysis of fluorescence decay data. *Rev. Sci. Instrum.* 62:47–52.

Fedchenia, I., and P.-O. Westlund. 1994. Influence of molecular reorientation on electronic energy transfer between a pair of mobile chromophores: the stochastic Liouville equation combined with Brownian dynamic simulation techniques. *Phys. Rev. E.* 50:555–565.

Förster, Th. 1948. Zwischenmolekulare Energiewanderung und Fluoreszenz. *Ann. Phys.* 2:55–75.

Haugland, R. P. 1996. Handbook of Fluorescent Probes and Research Chemicals, 6th Ed. Molecular Probes, Eugene, OR.

Ikeda, T., B. Lee, S. Kurihara, S. Tazuke, S. Ito, and M. Yamamoto. 1988. Time-resolved observation of excitation hopping between two identical chromophores attached to both ends of alkanes. *J. Am. Chem. Soc.* 110:8299–8304.

Johansson, L. B.-Å., F. Bergström, P. Edman, I. V. Grechishnikova, and J. G. Molotkovsky. 1996a. Electronic energy migration and molecular rotation within bichromophoric macromolecules. 1. Test of a model using bis(9-anthrylmethyl phosphonate)bisteroid. *J. Chem. Soc. Faraday Trans.* 92:1563–1567.

Johansson, L. B.-Å., P. Edman, and P. O. Westlund. 1996b. Energy migration and rotational motion within bichromophoric molecules. II. A derivation of the fluorescence anisotropy. *J. Chem. Phys.* 105: 10896–10904.

Kalman, B., A. Sandström, L. B-Å. Johansson, and S. Lindskog. 1991. Electronic energy transfer and fluorescence quenching in the active sites of mercuric reductase. *Biochemistry.* 30:112–117.

Karolin, J., L. B.-Å. Johansson, L. Strandberg, and T. Ny. 1994. Fluorescence and absorption spectroscopic properties of dipyrrometheneboron difluoride (BODIPY) derivatives in liquids, lipid membranes, and proteins. *J. Am. Chem. Soc.* 116:7801–7806.

Kaschke, M., N. P. Ernsting, B. Valeur, and J. Bourson. 1990. Subpicosecond time-resolved intramolecular electronic energy transfer in flexible bichromophoric coumarin molecules. *J. Phys. Chem.* 94:5757–5761.

Knutson, J. R., J. M. Beechem, and L. Brand. 1983. Simultaneous analysis of multiple fluorescence decays. *Chem. Phys. Lett.* 102:501–507.

Kronmal, R. A., and A. V. Peterson, Jr. 1979. On the alias method for generating random variables from a discrete distribution. *Am. Statist.* 33:214–218.

Lakey, J. J. H., D. Baty, and F. Pattus. 1991. Fluorescence energy transfer distance measurements using site-directed single cysteine mutants. *J. Mol. Biol.* 218:639–653.

Latt, S. A., H. T. Cheung, and E. R. Blout. 1965. Energy transfer. A system with relatively fixed donor-acceptor separation. *J. Am. Chem. Soc.* 87:995–1003.

Löfroth, J.-E. 1985. Deconvolution of single photon counting data with reference method and global analysis. *Eur. Biophys. J.* 13:45–58.

Marsaglia, G., and A. Zaman. 1987. Toward a random number generator. Florida State University Report FSU-SCRI-87-50.

Metropolis, N., A. W. Rosenbluth, M. N. Rosenbluth, and A. H. Teller. 1953. Equation of state calculations by fast computing machines. *J. Chem. Phys.* 21:1087–1092.

Moog, R. S., A. Kuki, M. D. Fayer, and S. G. Boxer. 1984. Excitation transport and trapping in a synthetic chlorophyllide substituted hemoglobin: orientation of the chlorophyll S_1 transition dipole. *Biochemistry.* 23:1564–1571.

Mottonen, J., A. Strand, J. Symersky, R. M. Sweet, D. E. Danley, K. F. Geoghegan, R. D. Gerard, and E. J. Goldsmith. 1992. Structural basis of latency in plasminogen activator inhibitor-1. *Nature.* 355:270–273.

Strandberg, L., J. Karolin, L. B.-Å. Johansson, M. Fa, S. Aleshkov, and T. Ny. 1994. Fluorescence studies on plasminogen activator inhibitor 1: reactive centre cysteine mutants remain active after fluorophore attachment. *Tromb. Res.* 76:253–267.

Stratikos, E., and P. G. W. Gettins. 1997. Major proteinase movement upon stable serpin-proteinase complex formation. *Proc. Natl. Acad. Sci. USA.* 94:453–458.

Stryer, L., and R. P. Haugland. 1967. Energy transfer: a spectroscopic ruler. *Proc. Natl. Acad. Sci. USA.* 58:719–726.

Valeur, B. 1989. Intramolecular excitation energy transfer in biochromophoric molecules—fundamental aspects. *In* Fluorescent Biomolecules. Methologies and Applications. D. M. Jameson and G. D. Reinhart, editors. Polonium Press, New York. 269–303.

Valeur, B., J. Muggier, J. Pouget, J. Bourson, and F. Santa. 1989. Calculation of the distribution of donor-acceptor molecules in flexible bichromophoric molecules. Application to intramolecular transfer of excitation energy. *J. Phys. Chem.* 87:6073–6079.

van Der Meer, B., G. Cooker, III, and S.-Y. S. Hen. 1994. Resonance Energy Transfer. VCH Publishers, New York.

Wilczynska, M., M. Fa, J. Karolin, P.-I. Ohlsson, L. B.-Å. Johansson, and T. Ny. 1997. New structural insights into native serpin-protease complexes reveal the inhibitory mechanism of serpins. *Nature Struct. Biol.* 4:354–357.